DALTON
FULL PAPER

Electron and energy transfer within dyads involving polypyridyl-ruthenium(II) and -osmium(II) centres separated by rigid alicyclic bridges

Laurence S. Kelso,[a] Trevor A. Smith,[b] Austin C. Schultz,[c] Peter C. Junk,[a] Ronald N. Warrener,[c] Kenneth P. Ghiggino[b] and F. Richard Keene*[a]

[a] *School of Biomedical and Molecular Sciences, James Cook University, Townsville, Queensland 4811, Australia*
[b] *Photophysics Laboratory, School of Chemistry, University of Melbourne, Parkville, Victoria 3052, Australia*
[c] *Centre for Molecular Architecture, Central Queensland University, Rockhampton, Queensland, 4702, Australia*

Received 19th April 2000, Accepted 12th June 2000
Published on the Web 13th July 2000

Rigid alicyclic frameworks (often referred to as molracs, relating to the molecular rack nature of the frame) have been used to vary the separation between organic electron-acceptor (quinone) moieties and chromophoric polypyridylruthenium(II) centres, and between metal centres in Ru–Ru and Ru–Os dinuclear complexes. Photophysical studies have allowed a preliminary insight into the effectiveness of such alicyclic structures in mediating intramolecular photoinduced energy and electron transfer. In the chromophore–spacer–quinone dyads, solvent-dependent quenching of the ruthenium(II) MLCT emission was observed and attributed to electron transfer processes. Distance and stereochemical dependencies of the quenching suggested that through-bond coupling was a factor in these systems. In the heterodinuclear systems, the photo-excited ruthenium(II) chromophore underwent intramolecular energy transfer to the osmium(II) component. A through-space Förster dipole–dipole mechanism could adequately account for the rate of the energy transfer process observed.

Introduction

Recent studies[1] have elegantly demonstrated the role of rigid spacer molecules in mediating both electron and energy transfer between organic redox-active donor and acceptor entities. A number of these donor and acceptor groups have also been used to quench the photo-induced excited states of transition metal complexes and porphyrinic systems.[2,3] Such intramolecular processes are of considerable interest as the chromophoric characteristics of metal centres have led to their incorporation into multi-component assemblies which attempt to mimic aspects of the photosynthetic process.[4,5]

To achieve prolonged photo-promoted charge separation within such arrays, an understanding of the communication between the components and its dependence on their spatial interrelationship is required. Significantly, we have reported on the triplet excited-state lifetimes of the four geometric isomers of a mononuclear ruthenium(II) complex possessing quencher-modified polypyridyl ligands.[6] In those studies, the quenchers were tethered to the 4 position of one of the pyridyl rings of a 2,2′-bipyridine moiety *via* a short, flexible alkyl chain. However, the system had a degree of conformational ambiguity because of flexibility within the linkage to the substituents.

Aromatic spacers and alkyne rods have provided a means of controlling the distances between the interacting centres of dimetallic species, but they allow rotational mobility around the axis of the link between the two components.[7] Rigid bridges are known, the most common type employing an extended series of fused aromatic rings,[8] which act as conduits between the component metal centres. In this category, there are a number of aromatic heterocyclic ligand bridges which maintain the metal centres in close proximity to each other. In systems of this type we have reported measurable differences between the physical characteristics of the diastereoisomers present in dinuclear and trinuclear complexes involving the bridging ligands apy/mapy {apy = 2,2′-azobis(pyridine); mapy = 2,2′-azobis(4-methylpyridine)}[9] and HAT (1,4,5,8,9,12-hexaazatriphenylene).[10] Rigid bridges incorporating non-conjugated alicyclic frameworks have also been reported, utilising adamantane rings[11] or polynorbornane units.[12,13] In principle, intercomponent communication in such structures may occur either *via* the carbon σ framework or "through space".

This final class of linkages provides a particular opportunity to further the understanding of the factors which control intramolecular electron and energy transfer. In the present study we have extended the work done on rigid space-separated organic systems by interposing a rigid saturated framework between a metal-based chromophore and an quencher unit on one hand, and between two metal-based chromophores on the other. Several other conformationally rigid ligands incorporating 1,10-phenanthroline, 4,5-diazafluorene and 3,6-di(2-pyridyl)pyridazine have also been reported.[13–16] However only limited photophysical data currently exist on the luminescent transition metal complexes prepared from such ligands.[11b,15,17] We now report the use of these systems to probe the effectiveness of alicyclic structures in mediating electron and energy transfer processes in inorganic systems, principally those based on d^6 polypyridyl metal complexes.

Results and discussion

Syntheses

The mononuclear chromophore–quencher dyads (**5** and **6**, Fig. 1) were prepared *via* an alicyclic coupling of the appropriate epoxycyclobutane complex precursors (**11** or **12**) with the norbornene-functionalised naphthaquinone **10**,[18] shown in Scheme 1. A single reaction product is generated in a stereo-

selective cycloaddition which involves ring opening of the epoxide to give a 1,3-dipolar intermediate. The newly formed complex comprises a Ru^{II} and a quinone unit, spatially separated by a rigid molrac (molecular rack) framework. The heterodinuclear complex dyads (**8** and **9**, Fig. 2) were obtained *via* an analogous coupling of the appropriate mononuclear precursors.

The ligand present in complex **5** could also be prepared *via* a coupling of the methanoanthraquinone **10** with the free epoxycyclobutane, however this synthesis (with subsequent attachment to the metal centre) proved to be a less efficient pathway than the corresponding reactions using the metal complex precursors. Preparation of rigid naphthaquinone-functionalised 1,10-phenanthroline ligands in pre-assembled form (without complexation) was only required for the shortest dyads (**3** and **4**). Alternative non-coupling approaches (involving protection and deprotection of the quinone) were generally unsuccessful.[19] While the bridged diphenanthroline ligands incorporated in the dinuclear complexes **8** and **9** could also be synthesized prior to complexation, their extreme insolubility made sequential co-ordination of two different metal centres virtually impossible.[18] Access to the heterodinuclear complexes was therefore only possible *via* coupling of the metal complex precursors.

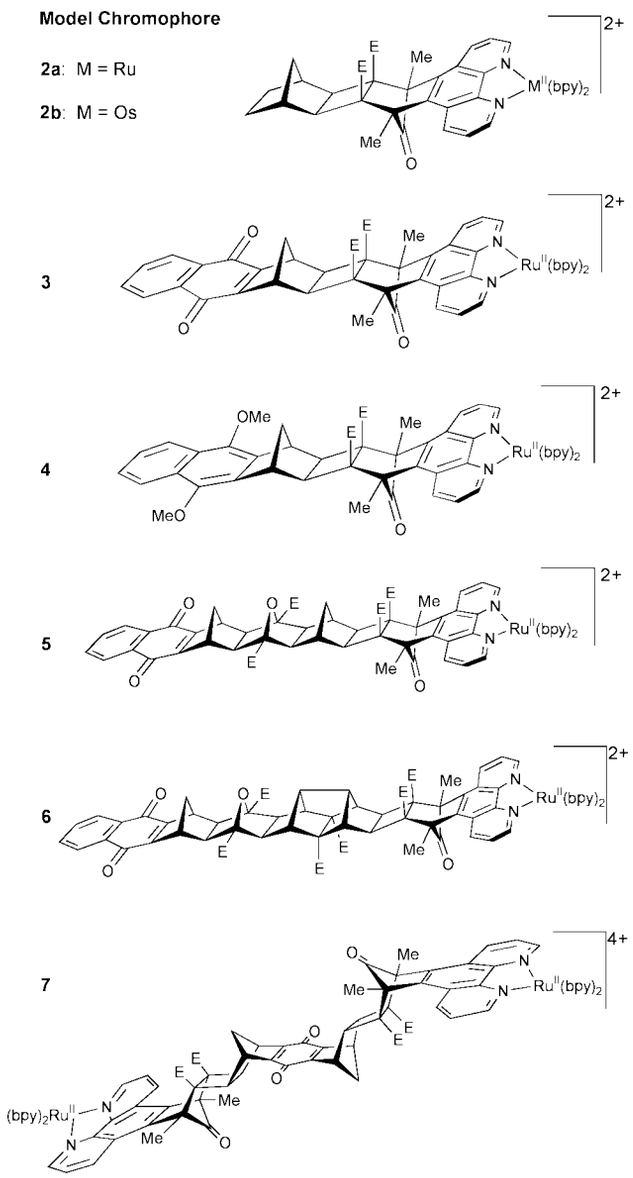

Fig. 1 "Chromophore–spacer–quencher" complexes possessing organic electron acceptor functionality {E = CO_2Me}.

Electronic absorption spectra

Electronic spectra were recorded in three different solvents (acetonitrile, dichloromethane and water), however no solvent dependency was observed for any of the dyads investigated. The UV/visible absorption spectra of the ruthenium(II) (**2a**) and osmium(II) (**2b**) model chromophores show intense absorptions in the UV region due to π–π* transitions of the bipyridine- and phenanthroline-type ligands, and in the visible region due to metal-to-ligand charge-transfer (MLCT) transitions. The Ru^{II}-based dyads (**3**–**6**) possess similar profiles, with additional features at 285 or 215 and 236 nm which are assigned to the molrac-modified naphthaquinone and dimethoxynaphthalene quenchers, respectively. These additional absorbances overlap substantially with the other ligand π–π* transitions. The heterodinuclear complexes (**8** and **9**) exhibit spectra in which

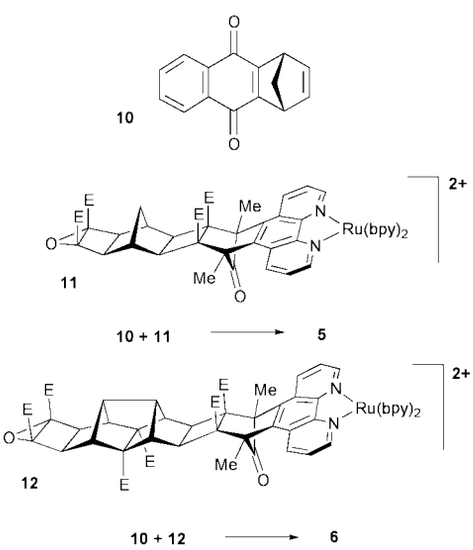

Scheme 1 Synthesis of dyads *via* Method B.

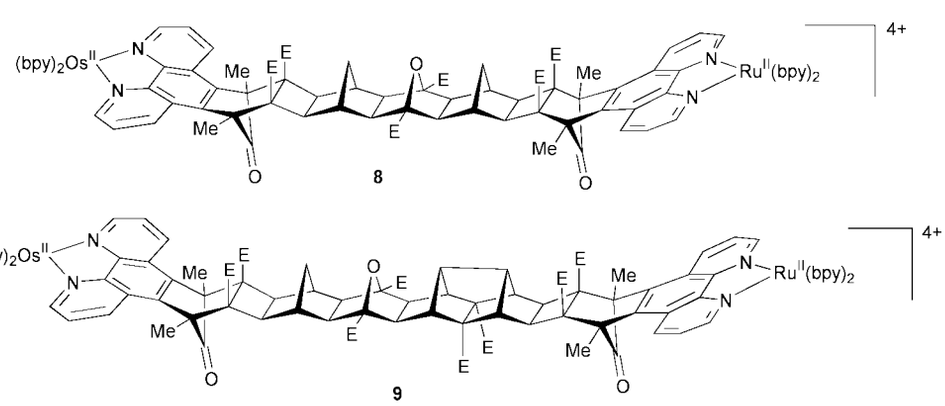

Fig. 2 Dinuclear species used in the energy transfer study.

the absorption coefficients are approximately the sum of those of the mononuclear model chromophores, and they display broad absorptions tailing out to >670 nm due to the osmium(II) MLCT transition. The ability of osmium centres to undergo spin–orbit coupling,[20] together with overlap of the characteristic long-wavelength absorption of the polypyridylosmium moiety with the emission of the polypyridylruthenium centres, makes these dyads good candidates for energy transfer studies.[21]

Electrochemistry

The model compounds **2** possessed well defined reversible redox couples associated with the oxidation of the respective metal centres. The mononuclear complex dyads **3**–**6** with organic quencher-modified ligands displayed a second reversible couple at either $E_{1/2} = ca.$ −965 or +780 mV (CH_3CN) which are assigned to the quinone reduction ($Q^{0/-1}$; **3**, **5**, and **6**) or the dimethoxynaphthalene oxidation ($DMN^{+1/0}$; **4**), respectively. Further ligand-based reductions occurred at more cathodic potentials, but upon re-oxidation sharp desorption peaks were observed. The reductions arise from ligand-based processes,[22] but the desorption peaks presumably arise from the presence of ester O-methyl substituents on the bridge superstructure, since the feature was not observed in complexes containing ligands in which those substituents were absent. Electrochemical measurements in dichloromethane and water (unbuffered and buffered at pH 9.2) showed minimal shifts (≤85 mV) in the redox couple of naphthoquinone, with a complementary shift (30 mV) in the $Ru^{III/II}$ couple. The heterodinuclear complexes **8** ($E_{1/2}$ = 0.995, 0.552 V)[18] and **9** ($E_{1/2}$ = 1.000, 0.555 V)[18] displayed two one-electron waves corresponding to successive $Ru^{III/II}$ and $Os^{III/II}$ oxidations. The redox couples associated with these metal-based processes were not shifted relative to the model chromophores, which implies that there is limited electronic coupling across the alicyclic frameworks.

Crystal structure of model ligand and geometry optimisations

Attempts to obtain crystals of the dyads suitable for crystal structure determination were unsuccessful. However, a structure was obtained for the molrac-modified phenanthroline ligand **1** used in the model chromophore complexes **2**, which is shown in Fig. 3. Using the parameters obtained, intercomponent distances and interplanar angles were calculated from geometry-optimised structures (Figs. 4(a) and 4(b)), using a combination of the semi-empirical AM1 and PM3(tm) force fields for the respective ligands and dyad complexes. Comparison of the crystallographic coordinates of **1** with the AM1-calculated values shows excellent agreement (RMS differences between bond lengths, bond angles and torsion angles between the AM1 calculated values for the "free" ligand and the crystal structure values were 0.021 Å, 1.9 and 3.6° respectively). The PM3(tm)-determined coordinates for the same ligand within the model ruthenium complex (**2a**) also compared well with those of the free form (RMS differences between bond lengths, bond angles and torsion angles between the PM3(tm) calculated values for the complex **2a** and the crystal structure values for the ligand were 0.018 Å, 1.7 and 3.6°, respectively). Such correlations are to be expected for these conformationally rigid structures since the use of computational techniques for determining interatomic distances and angles in organic rigidly bridged dyads is well established.[22,24] The two planes inscribed by (ϕ) are the central aromatic ring of the phenanthroline and the quinonoid ring at each end of the molrac structure for the mononuclear complexes, and between the two central phenanthroline rings for the heterodinuclear complexes. The straight line distance (d) is a through-space displacement between the centre of the quinonoid ring and the metal centre for Fig. 4(a), and between the two metal centres in Fig. 4(b).

The alicyclic frameworks that link the chromophore and quencher components within a dyad are not planar. Geometry

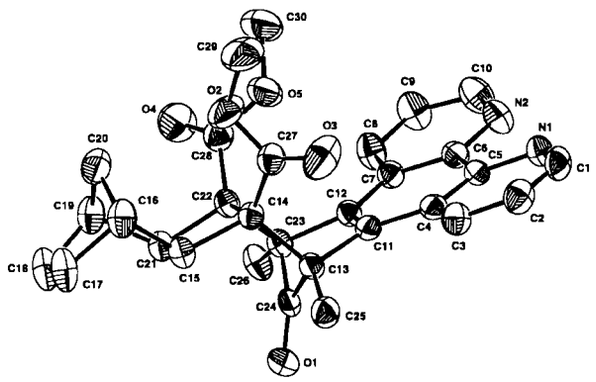

Fig. 3 An ORTEP[23] diagram of the crystal structure of ligand **1**.

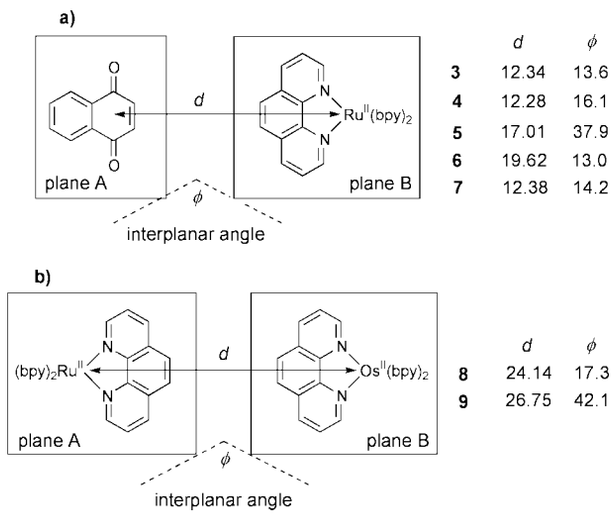

	d	φ
3	12.34	13.6
4	12.28	16.1
5	17.01	37.9
6	19.62	13.0
7	12.38	14.2

	d	φ
8	24.14	17.3
9	26.75	42.1

Fig. 4 Intercomponent displacement (Å) and angles (°) within dyads studied.

optimisations (AM1) show significant variations in the degree of curvature between each of the rigid ditopic ligands used in this study (Fig. 5). Judicious choice of the type of molrac subunit allows synthetic control over the intramolecular orientation and displacement of each component. As an example, the inclusion of a bridge-linked sesquinorbornane subunit in dyads **6** and **9**[18] produces a more planar framework[24] than is present in dyads **5** or **8**, which comprise only norbornane, cyclobutane and oxanorbornane units (Figs. 4 and 5). Accordingly, the through-space displacement between the two components of each dyad studied is considerably less than any through-bond value. Since these molrac structures contain σ bonds in a predominantly *trans* configuration, any through-bond interactions were analysed in terms of the number of aliphatic C–C bonds separating the two redox-active ends of the molecule.

Photophysical studies

A recent photophysical study[17] reported electron transfer processes in ruthenium complexes of dipyridoquinoxaline ligands linked to benzoquinone or naphthoquinone functionalities *via* a specific six-bond norbornyl-type moiety. Energy transfer was also observed in a dinuclear (Ru–L–Os) complex involving a bridge comprising two dipyridoquinoxaline ligating groups joined by the same linkage.[17] In the present study, variation of the alicyclic linkage has allowed assessment of the effects of orientation and relative displacement of the components in the transfer processes, and also the effect of solvent variation has been probed. It should also be noted that the ligand quencher and ligand bridges do not involve N-heterocycle moieties in the spacer: in earlier studies involving ligands such as dppz {dipyrido[3,2:*a*-2′,3′:*c*]phenazine}, these have been shown to

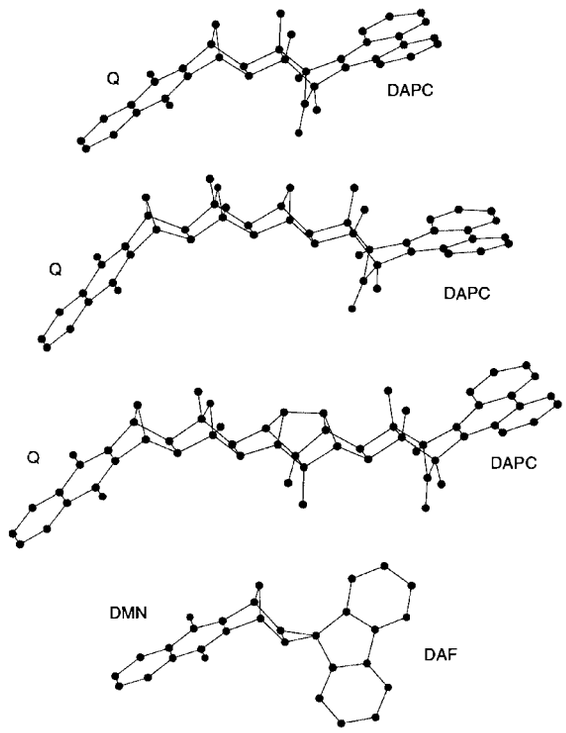

Fig. 5 Calculated structures (AM1) of some representative ligands present in the mononuclear complexes used in this study. Hydrogen atoms and methyl ester groups have been omitted for the sake of clarity {DAF = 4,5-diazafluorene; DAPC = 7,8-diazaphencyclone; DMN = 1,4-dimethoxynaphthalene; Q = 1,4-naphthaquinone}.

affect the photophysical behaviour because of protonation reactions.[26,27]

Comparative model complexes were prepared that were structurally similar to the metal-based norbornyl-modified chromophoric units in each of the dyads investigated. The luminescence of the ruthenium(II) model compound **2a** has a maximum at 610 nm (Fig. 6) and a lifetime in the range 1–2 μs, dependent on the solvent (Table 1). This was 40–50% longer than the lifetimes[20] of the classical polypyridylruthenium chromophores $[Ru(bpy)_3]^{2+}$ and $[Ru(bpy)_2(phen)]^{2+}$, and implied that the presence of a molrac-modified ligand in these types of complexes stabilises the resulting ^{3}MLCT excited state. This may arise from an increased rigidity in the overall complex leading to a decrease in the non-radiative (k_{nr}) component associated with competing thermally activated processes.[28] This was supported by the observation that under conditions where no luminescence quenching was observed the larger (more rigid) complex dyads exhibited slightly longer lifetimes than the smaller, structured model complex.

Comparison of the luminescence lifetime data for the mononuclear complexes investigated (Table 1) points to some interesting relationships between the degree of quenching, solvent polarity and the intercomponent displacement within these systems. The initial studies carried out in CH_3CN solution at 293 K gave a luminescence lifetime of 1.36 ± 0.01 μs for the model compound, **2a**. Excitation of the shortest dyad system (**3**) at 452 nm led to a large reduction in the luminescence intensity relative to the model (Fig. 6) and a corresponding decrease in the lifetime of this emission to 56 ± 0.5 ns. This implies the existence of a competing non-radiative process, which we believe to be electron transfer (et) to the quinone quencher located some 12.3 Å from the metal-based chromophore. No evidence was observed in this solvent for any quenching in the dyads where the quinone was more remote from the metal centre (dyads **5** and **6**). When the measurements were repeated in a less polar solvent (CH_2Cl_2) no appreciable quenching of

Table 1 Luminescence decay lifetimes of dyads studied in various solvents at 293 K. Also shown are the calculated rates of electron transfer for the series of naphthaquinone dyads in water $\{k_{et} = (1/\tau_{dyad}) - (1/\tau_{2a})\}$

	τ/ns			
Complex	CH_3CN	CH_2Cl_2	Water	k_{et} (water)/10^6 s^{-1}
2a	1360	970	1850	
3	56	907	<5	>200
4	1440		1900	
5	1530		190	4.72
6	1400		1550	0.105
7	1540			
8	49			
9	105			

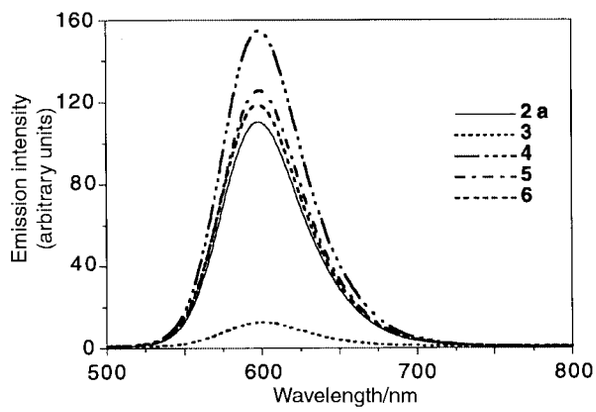

Fig. 6 Emission spectra of dyads and model chromophore at 293 K in CH_3CN.

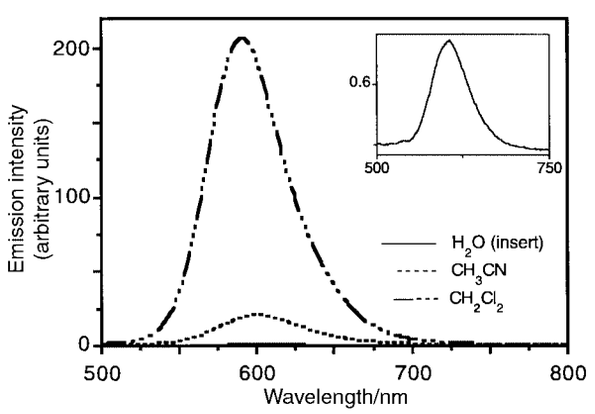

Fig. 7 Comparative emission spectra of compound **3** in different solvents at 293 K.

the triplet excited state was observed in any dyad (including the shortest).

In water (the most polar solvent used) the lifetime of the model **2a** increased to 1.85 ± 0.08 μs. However, for dyad **3** the residual luminescence became almost undetectable (Fig. 7) and the emissive lifetime shortened to <5 ns (the resolution limit of the instrumentation). The lifetimes of dyads **5** and **6** also appeared to shorten relative to the model **2a** following excitation (in water), albeit less dramatically than **3**. Conversely dyad **4**, which has the same molrac structure as that of **3** except that the quinone has been replaced with a dimethoxynaphthalene (DMN) unit, displayed no evidence of mediating electron transfer under any of the solvent regimes and had a slightly longer lifetime relative to the model chromophore.

The Weller equation[29] can be used to estimate the driving force (ΔG) for electron transfer in these systems, Eqns. (1)

and (2), E_{ox}(D) and E_{red}(A) are the redox potentials of the donor

$$\Delta G = E_{ox}(D) - E_{red}(A) - E_{00} - X \quad (1)$$

$$X = 14.45 q_1 q_2 / \varepsilon R_c \quad (2)$$

and acceptor respectively, E_{00} is the zero–zero excitation energy and X is a modifying term to account for the finite donor–acceptor separation (R_c) between the ions with charges q_1 and q_2 in a solvent of relative permittivity ε. The absorption and emission maxima of these systems appear to be solvent independent (see details given in the Experimental section), and the zero–zero excitation energy (E_{00}) can be estimated from the emission maxima of related complexes recorded in a low temperature glass to be approximately 2.16 eV.[17] Using the electrochemical data, ΔG in acetonitrile for compound **3** is calculated to be approximately −0.10 V indicating that photoinduced electron transfer is thermodynamically favoured. The rates of electron transfer calculated (Table 1) will be influenced by the electronic coupling between the donor and acceptor (*i.e.* overlap of the donor and acceptor wavefunctions either through space or through the linking framework) and the Franck–Condon factors (reaction free energy, reorganisation energy). The trend of decreasing excited state lifetimes with increasing solvent polarity in those systems undergoing some form of quenching lends support to our contention that an electron transfer rather than an energy transfer phenomenon is operative.[30] It is of interest to compare the quenching behaviour observed in the molrac-modified polypyridylruthenium(II) complexes with similar bridged organic electron donor/acceptor dyads where through-bond electron transfer has been observed (in CH_3CN and less polar solvents) over quite large distances.[12a,31] ^{3}MLCT excited states in d^6 metal-based systems are very different to both the singlet and/or triplet states of the various organic donor/acceptor molecules studied previously, and hence any comparison of the solvent reorganisation energy (λ) and the associated free energy change (ΔG) is not straightforward. In the organic dyads an exponential relationship ($k_{et} \propto \exp(-\beta n)$) between the electron transfer rate constant, k_{et}, and the number of C–C σ bonds, n, in the linking bridge has been postulated.[4,12a] A value for the attenuation coefficient, β, of approximately one has been observed experimentally in many organic donor/acceptor systems. The calculated rates of electron transfer in water (Table 1) in the present series of naphthaquinone molecules (compounds **3**, **5** and **6**) as a function of the inter-chromophore distances given in Fig. 4 provide confirmation that the attenuation of the electron transfer rate with distance is very close to unity ($Å^{-1}$) in this series of inorganic donor/organic acceptor compounds (Fig. 8). The observation that electron transfer occurs over distances exceeding the direct spatial orbital overlap of the donor and acceptor and the similarity in attenuation coefficient suggest that electron transfer is also mediated by a through-bond interaction in the molecules studied here.

The lack of any luminescence quenching, or shortening of the residual lifetime, of dyad **4** was expected, since no quenching of the ^{3}MLCT emission was observed in previous low temperature studies (77 K) of polypyridylruthenium(II) complexes incorporating norbornyl DMN-modified 4,5-diazafluorene ligands (DAF; Fig. 5). In addition, for the case of DAF the orthogonality of the ligating unit relative to the quencher moiety (Fig. 5) may also reduce the through-bond coupling between the redox couples. Previous work using organic donor–acceptor polynorbornyl systems has unequivocally established the importance of orientation and stereochemistry within the alicyclic framework as a major influence on bond-mediated electron transfer processes.[1d,12a,30] Paddon-Row *et al.* have shown that through-bond coupling is maximised for an antiperiplanar arrangement of relaying σ bonds (the so-called "all-*trans* rule").[32] The absence of luminescence

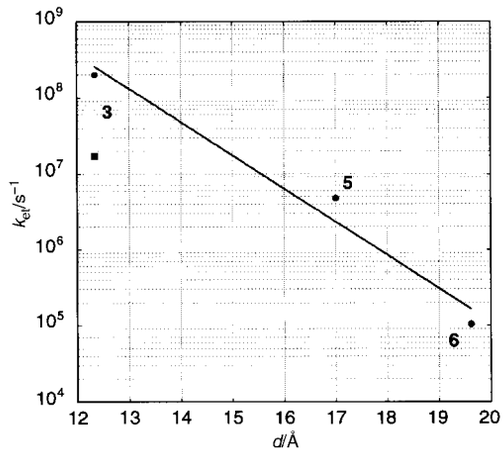

Fig. 8 Semi-log plot of k_{et} *vs.* donor–acceptor distance (Å) for the naphthaquinone series of compounds (**3**, **5** and **6**) in water (●). The solid line is an exponential fit with slope of unity. The point for compound **3** in acetonitrile is also given (■).

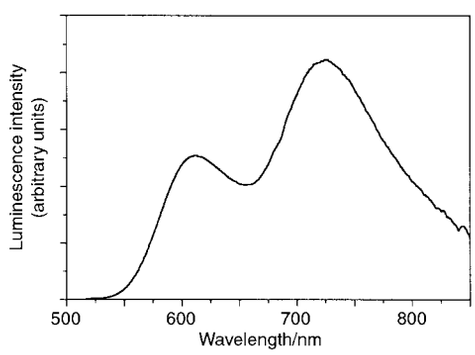

Fig. 9 Emission spectrum (corrected) for dyad **8** at 293 K in CH_3CN.

quenching in triad **7** is also interesting since the bridging framework between each of the two metal-centred chromophores and the central quinone is identical to that in **3**. Structurally, however, this quinone is quite different to the terminal acceptors of the other systems studied and this is reflected in the $Q^{0/-1}$ redox couple, which is ≈200 mV more anodic relative to the mononuclear dyads.

The Ru^{II}-based luminescence of the two large heterodinuclear complexes (**8** and **9**) was quenched to an extent greater than 95% relative to the model compound **2a** following excitation at 452 nm. The reduction in emission intensity at 610 nm (due to the Ru^{II}-based MLCT emission) was accompanied by a stronger emission at 727 nm (Fig. 9), which can be assigned to an osmium(II) MLCT excited state. This indicates that energy is being transferred from the ruthenium chromophore to the osmium chromophore in each molecule. There is a significant overlap of the $[Ru(bpy)_2(L)]^{2+}$ (donor) emission spectrum with the $[Os(bpy)_2(L)]^{2+}$ absorption profile (Fig. 10), which is a requirement for Förster dipole–dipole energy transfer.[33] Although this mechanism is usually applied to singlet excited states, the well known proclivity of d^6 metal complexes to possess "mixed character" has permitted its extended application to energy transfer processes within metal-based supramolecular systems also.[34] Assuming such a mechanism to be appropriate, the Förster critical transfer distance, R_o, can be calculated using[35] eqn. (3). The spectral overlap term, J, was

$$R_0^6 = 9000(\ln(10)\kappa^2 \phi_{D_f} J / 128\pi^5 n^4 N_{AV}) \quad (3)$$

calculated using the emission and absorption spectra of the model compounds (**2a** and **2b** respectively) to be 6.03×10^{-14} M^{-1} cm^3 which is in close agreement with the value reported by Furue *et al.*[36] for related compounds. The emission quantum yield of the ruthenium model compound, ϕ_{D_f}, was

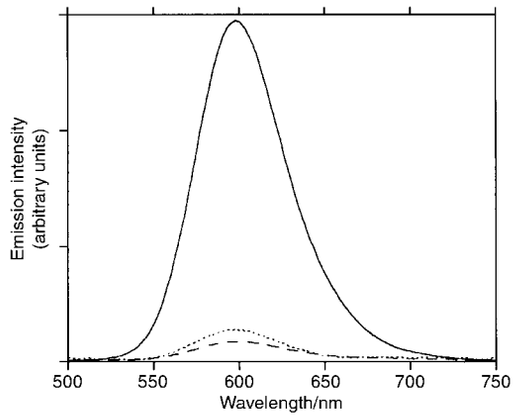

Fig. 10 Emission spectra of the ruthenium model compound **2a** (——), and dinuclear Ru–Os complexes **8** (-----) and **9** (·····) in acetonitrile solution at 293 K.

taken to be 0.07. The actual value of the R_o is influenced by the orientation factor (κ^2) which can vary from 0 to 4 and the appropriate value of this term for the current molecules has not been determined. If κ^2 is taken to be 2/3 (which is only correct for a random ensemble), the R_o is calculated to be 30.2 Å. This is somewhat larger than that reported recently by Balzani *et al.*,[37] for related molecules but is in close agreement with that reported by Furue *et al.*[36] The efficiency of energy transfer, E_{et}, given by: $E_{et} = R_0^6/(R_0^6 + r^6)$, where r is the donor–acceptor separation, can then be determined. The rate of energy transfer, k_{et}, can also be calculated using the relationship: $k_{et}\tau_D^{-1} = (R_0/r)^6$ where τ_D is the lifetime of the donor emission in the absence of energy transfer. PM3(tm) calculations determined the metal–metal displacements of the Ru–Os dyads investigated to be 24.1 and 26.7 Å, resulting in estimates for E_{et} of 79.6 and 67.9% respectively, assuming R_o to be 30.2 Å. These calculated efficiencies can be compared with the luminescence quenching observed experimentally (Fig. 10), which shows ≈94% quenching of the ruthenium emission in the heterodinuclear complex with the shorter bridge (**8**) and ≈91% for the complex (**9**) with the longer bridge. Similarly, energy transfer rates of 2.85×10^6 and 1.54×10^6 s^{-1} are estimated, which can be compared to with the observed rates of 19.7×10^6 and 8.8×10^6 s^{-1} respectively. As mentioned above, the R_o value, and hence the calculated transfer efficiencies and energy transfer rates, are influenced by the κ^2 term and this may account for the discrepancies between the calculated and observed values for these parameters. For example, if κ^2 is set to its maximum possible value of 4, the calculated efficiencies and rates become 95.9 and 92.7% and 17.1×10^6 and 9.23×10^6 s^{-1} respectively which are in excellent agreement with those observed. These results suggest that the Förster mechanism is largely responsible for the energy transfer observed.

Unlike the mononuclear complexes discussed above, the emission intensity and lifetimes of the dinuclear species were largely independent of solvent. This supports our contention that the quenching process in these very large space-separated dimetallic molecules involves non-radiative energy transfer rather than electron transfer phenomena.

Conclusion

The use of rigid alicyclic frameworks to link organic electron-acceptor moieties to chromophoric polypyridylruthenium(II) centres has allowed a preliminary insight into the effectiveness of molrac structures in mediating the charge-transfer process. In chromophore–quencher dyads involving quinone electron acceptors efficient quenching of the ruthenium(II) MLCT excited state was observed. The solvent dependency of this process, together with the steep distance dependence, suggests that through-bond coupling is a factor in the systems studied.

We have also shown that alicyclic frameworks are effective in bridging heterodinuclear species and that the ruthenium(II) chromophore within these molecules is quenched *via* an intramolecular energy transfer to the osmium(II) component. The results indicate that the Förster dipole–dipole process is the major energy transfer mechanism.

Experimental

Physical measurements

Instrumentation and conditions used for spectral (UV/visible, 300 MHz ^{1}H NMR) and electrochemical measurements {cyclic voltammetry (CV) and differential pulse voltammetry (DPV)} have been described previously.[9] Microwave reactions were conducted in a modified 600W Sharp Carousel R-2V55 microwave oven. High-resolution mass spectra were recorded on a Micromass Autospec magnetic sector instrument with an electrospray source: samples were run in acetonitrile solution using polyethylene glycol intrinsic standards.

Uncorrected emission spectra were recorded using a Hitachi 4010 spectrofluorimeter. A SPEX Fluorolog spectrofluorimeter was used to obtain corrected emission spectra beyond 600 nm. Luminescence decay lifetimes were measured using a nitrogen laser (Laser Photonics LN300C)/digital oscilloscope system (Tektronix TDS520). All samples were degassed using repeated freeze–pump–thaw cycles prior to excitation. The concentration of solutions used for the room temperature emission experiments was typically $(1–3) \times 10^{-5}$ M.

The geometry of each dyad was determined *via* semi-empirical {AM1 and PM3(tm)} geometry optimisations using the SPARTAN program[38] on a SGI Power Challenge XL computer.

Materials

2-Methoxyethanol (puriss; Fluka) and NaCl (AR, Ajax) were used as supplied. Spectral grade dichloromethane (Univar) or acetonitrile (Sigma) were used for all spectroscopic and electrochemical measurements. All other reagent grade solvents were used without further purification.

Ligand syntheses

Ligand 1 (used in model complexes 2). A solution of 7,8-dihydrocyclobutene-1,2-diester[39] (100 mg, 423 mmol) and 7,8-diazaphencyclone[14b] (DAPC; 100 mg, 385 mmol) in chloroform (5 cm^3) was heated to 95 °C for 18 h in a sealed tube. The reaction solvent was removed under reduced pressure and the resultant solid separated by column chromatography on silica, eluting with methanol (1.5%)–chloroform. Combined fractions of the product (R_f 0.2) were evaporated to dryness to give a crystalline powder. The solid was recrystallised from dichloromethane–ethyl acetate to give the desired product as colourless crystals. Yield 148 mg (76%); mp 284 °C (decomp.). ^{1}H NMR (300 MHz, $CDCl_3$): δ 9.32 (dd, $J = 4.4$, 1.6, 2 H); 8.66 (dd, $J = 8.5$, 1.6, 2 H); 7.75 (dd, $J = 8.5$, 4.4, 2 H); 3.17 (s, 6 H); 2.57 (s, 2 H); 2.17 (s, 2 H); 2.07 (s, 6 H); 1.89 (d, $J = 11.1$, 1 H); 1.58 (m, 2 H); 1.28 (d, $J = 11.1$ Hz, 1 H) and 1.14 (m, 2H). ^{13}C NMR (75 MHz, $CDCl_3$): δ 200.73, 168.93, 149.69, 146.21, 135.26, 132.12, 125.37, 122.57, 62.16, 59.56, 51.14, 43.20, 37.73, 35.08, 28.22 and 9.49. Calc. for $C_{30}H_{28}N_2O_5$: C, 72.6; H, 5.68; N, 5.6. Found: C, 72.2; H, 5.67; N, 5.5%.

Synthesis of the space-separated ditopic ligands present in complexes **3**, **4** and **7** (Fig. 1) have been reported previously.[14c] The 1,10-phenanthroline-functionalised norbornene[14c] and epoxycyclobutanes[18,40] required as precursors in the syntheses of complexes **5**, **6**, **8**, and **9** (using Method B, below) have also previously been reported.

Complex syntheses

The precursor complexes $[Ru(bpy)_2(CF_3SO_3)_2]$[41] and $[Os(bpy)_2(CF_3SO_3)_2]$[18] were prepared using literature methods. The complex dyads used in this study were prepared using one of two different approaches.

Method A. Complexes **3**, **4**, and **7**, as well as the model chromophores **2**, were synthesized from the appropriate ligand and an excess of $[M(bpy)_2(CF_3SO_3)_2]$. In a typical reaction, the 1,4-dimethoxynaphthalene-functionalised phenanthroline[14b,c] (25 mg; 0.038 mmol) was dissolved in chloroform (2 cm^3), the ligand solution diluted 50% by the addition of 2-methoxyethanol, and $[Ru(bpy)_2(CF_3SO_3)_2]$ (50 mg, 0.069 mmol) added. The mixture was refluxed for 5 min in a microwave oven, during which time it turned from burgundy to bright orange. After evaporation of the solvent, the residue was purified by cation-exchange chromatography {SP-Sephadex C-25; eluent acetone–water 30 : 70 (0.25 M NaCl)}. The product was precipitated as the PF_6^- salt by addition of a saturated solution of KPF_6 to the orange eluent solution. Complete precipitation was only achieved after removal of the acetone *via* slow evaporation over several days. The orange solid was collected, washed with diethyl ether and air dried. Complex **2a**: yield 39.6 mg (87%). Accurate mass: observed *m*/*z* 1055.2063 (most abundant isotope peak within cluster), $[RuC_{50}H_{44}N_6O_5(PF_6)]^+$ requires 1055.2070. ^{1}H NMR (300 MHz, CD_3CN): δ 8.81–8.75 (m; 2 H), 8.55–8.45 (m; 4 H), 8.12–7.94 (m; 6 H), 7.83–7.79 (m; 2 H), 7.73–7.63 (m; 2 H), 7.48–7.38 (m; 4 H), 7.26–7.17 (m; 2 H), 3.26 (s; 3H), 3.00 (s; 3 H), 2.52 (br s; 2 H), 2.22 (s; 2 H), 2.10 (d; J = 9.0; 1 H), 2.04 (s; 3 H), 2.02 (s; 3 H), 1.55 (d; J = 7.5; 2 H), 1.25 (d; J = 11.4; 1 H) and 1.14 (d; J = 7.2 Hz; 2 H). UV/visible spectrum {CH_3CN; λ_{max}/nm ($10^{-4}\varepsilon$ (M^{-1} cm^{-1})}: 251 (4.71), 276 (6.56), 286 (6.32), 435(sh) (1.46) and 451 (1.62). Electrochemistry (DPV, platinum working electrode, reference Ag–Ag^+): {CH_3CN–0.1 M $[(n\text{-}C_4H_9)_4N]ClO_4$}, $E_{1/2}$ = 0.985 V; {dichloromethane–0.1 M $[(n\text{-}C_4H_9)_4N]ClO_4$}, $E_{1/2}$ = 1.020, −1.620 V; {water–0.1 M Na_2SO_4}, $E_{1/2}$ = 0.990 V. Complex **2b**: yield 92%. Accurate mass: observed *m*/*z* 1145.2661 (most abundant isotope peak within cluster), $[OsC_{50}H_{44}N_6O_5(PF_6)]^+$ requires 1145.2634. ^{1}H NMR (300 MHz, CD_3CN): δ 8.59–8.43 (m; 6H), 8.03 (d; J = 5.4; 1 H), 7.92–7.87 (m; 3 H), 7.83–7.70 (m; 4 H), 7.65–7.55 (m; 2 H), 7.36–7.29 (m; 4 H), 7.17–7.08 (m; 2 H), 3.27 (s; 3H), 3.00 (s; 3 H), 2.53 (br s; 2 H), 2.23 (s; 2 H), 2.08 (d; J = 9.2; 1 H), 2.05 (s; 3 H), 2.03 (s; 3 H), 1.55 (d; J = 7.5; 2 H), 1.25 (d; J = 11.1; 1 H) and 1.14 (d; J = 7.0 Hz; 2H). UV/visible spectrum {CH_3CN; λ_{max}/nm ($10^{-4}\varepsilon$/(M^{-1} cm^{-1})}: 251 (4.87), 279 (6.52), 290 (6.77), 434 (1.55) and 480 (1.60). Electrochemistry {DPV; CH_3CN–0.1 M $[(n\text{-}C_4H_9)_4N]ClO_4$; platinum working electrode; reference Ag–Ag^+}, $E_{1/2}$ = 0.560 V. Complex **3**: yield 65%. Accurate mass: observed *m*/*z* 1183.2008 (most abundant isotope peak within cluster), $[RuC_{58}H_{44}N_6O_7(PF_6)]^+$ requires 1183.1970. ^{1}H NMR (300 MHz, CD_3CN): δ 8.79 (m; 2 H), 8.55–8.45 (m; 4 H), 8.15–7.95 (m; 8 H), 7.84–7.66 (m; 6 H), 7.49–7.40 (m; 4 H), 7.28–7.17 (m; 2 H), 3.90 (s; 2 H), 3.35 (s; 3 H), 3.09 (s; 3 H), 2.32 (s; 2 H), 2.08 (d; J = 9.8; 1 H), 2.05 (s; 3 H), 2.02 (s; 3 H) and 1.72 (d; J = 10.2 Hz; 1H). UV/visible spectrum {λ_{max}/nm ($10^{-4}\varepsilon$/(M^{-1} cm^{-1})}: (CH_3CN) 252 (6.22), 275 (6.97), 284(sh) (6.32), 435(sh) (1.36) and 451 (1.50); (dichloromethane) 254 (5.66), 277 (6.54), 285(sh) (6.08), 437(sh) (1.26) and 453 (1.41); (water): 253 (5.12), 276 (5.84), 285 (5.54), 437(sh) (1.19) and 452 (1.26). Electrochemistry (DPV, platinum working electrode, reference Ag–Ag^+): {CH_3CN–0.1 M $[(n\text{-}C_4H_9)_4N]ClO_4$}, $E_{1/2}$ = 1.000, −0.970 V; {dichloromethane–0.1 M $[(n\text{-}C_4H_9)_4N]ClO_4$}, $E_{1/2}$ = 1.020, −0.1010 V; {water–0.1 M $[(n\text{-}C_2H_5)_4N]Cl$}, $E_{1/2}$ = 0.990, −0.925 V. Complex **4**: yield 88%. Accurate mass: observed *m*/*z* 1213.2432 (most abundant isotope peak within cluster), $[RuC_{60}H_{50}N_6O_7(PF_6)]^+$ requires 1213.2443. ^{1}H NMR (300 MHz, CD_3CN): δ 8.81 (dd; J = 9.0, 1.8; 2 H), 8.56–8.45 (m; 4 H), 8.15–7.94 (m; 4 H), 7.84–7.79 (m; 2 H), 7.76–7.66 (m; 2 H), 7.57 (d; J = 8.1; 2 H), 7.51–7.41 (m; 6 H), 7.29–7.24 (dd; J = 6.3, 1.1; 2 H), 7.20–7.12 (m; 2 H), 4.14 (s; 2 H), 4.00 (s; 6 H), 3.36 (s; 3 H), 3.11 (s; 3 H), 2.34 (s; 2 H), 2.29 (d; J = 8.9; 1 H), 2.05 (s; 3 H), 2.03 (s; 3 H) and 1.78 (d; J = 11.4 Hz; 1H). UV/visible spectrum {CH_3CN; λ_{max}/nm ($10^{-4}\varepsilon$/M^{-1} cm^{-1}}: 215 (5.31), 236 (6.39), 276 (5.16), 286 (5.10), 431(sh) (1.08) and 451 (1.21). Electrochemistry {DPV; CH_3CN–0.1 M $[(n\text{-}C_4H_9)_4N]ClO_4$; platinum working electrode; reference Ag–Ag^+}, $E_{1/2}$ = 0.990, 0.780 V. Complex **7**: yield 71%. Accurate mass: observed *m*/*z* 1079.1715 (most abundant isotope peak within cluster), $[Ru_2C_{102}H_{80}N_{12}O_{12}(PF_6)_2]^{2+}$ requires 1079.1717. ^{1}H NMR (300 MHz, CD_3CN): δ 8.78 (m; 4 H), 8.56–8.45 (m; 8 H), 8.15–7.94 (m; 12 H), 7.83–7.66 (m; 8 H), 7.49–7.41 (m; 8 H), 7.28–7.17 (m; 4 H), 3.74 (s; 4 H), 3.33 (s; 6 H), 3.08 (s; 6 H), 2.22 (s; 4 H), 2.08 (d; J = 4.2; 2 H), 2.04 (s; 6 H), 2.02 (s; 6 H) and 1.62 (d; J = 9.9 Hz; 2H). UV/visible spectrum {CH_3CN; λ_{max}/nm ($10^{-4}\varepsilon$/M^{-1} cm^{-1}}: 251 (8.79), 276 (11.56), 286 (11.45), 434 (sh) (2.57) and 451 (2.85). Electrochemistry {DPV; CH_3CN–0.1 M $[(n\text{-}C_4H_9)_4N]ClO_4$; platinum working electrode; reference Ag–Ag^+}, $E_{1/2}$ = 0.990, −0.735 V.

The norbornene–Os^{II} and the epoxycyclobutane–Ru^{II} precursors (**11** and **12**) used in the coupling reactions described below were also prepared *via* method A.

Method B. Compounds **8** and **9** were assembled using a convergent approach as reported previously.[42] Complexes **5** and **6** were prepared using the same coupling protocol in which a methanoanthraquinone **10**[14c,18] was coupled to a mononuclear ruthenium(II) precursor complex containing the appropriate phenanthroline-functionalised epoxycyclobutane ligand (Scheme 1).[18] In a typical reaction the complex (25 mg; PF_6^- salt)[18] and a small excess of the methanoanthraquinone[40] (8 mg) were heated for 16 h in a sealed tube (140 °C) in the minimum volume of acetonitrile–dichloromethane (2 : 1). The mixture was washed from the tube with acetone and added to water, giving a suspension which was extracted with diethyl ether to remove the unchanged quinone. The complex was purified by cation exchange chromatography as described above and isolated as the PF_6^- salt. Complex **5**: yield 21.2 mg (73%). HR-EIMS: *m*/*z* 1434.3 (16), $[M - PF_6]^+$; 644.7 (100), $[M - 2PF_6]^{2+}$; and 337.3 (63), $[Ru(bpy)_2(DAPC)]^{2+}$. Accurate mass: observed *m*/*z* 1433.2817 (most abundant isotope peak within cluster), $[RuC_{71}H_{58}N_6O_{12}(PF_6)]^+$ requires 1433.2824. ^{1}H NMR (300 MHz, CD_3CN): δ 8.73 (m; 2H), 8.54–8.44 (m; 4 H), 8.11–7.96 (m; 8 H), 7.82–7.62 (m; 6 H), 7.47–7.35 (m; 4 H), 7.25–7.16 (m; 2 H), 3.91 (s; 3 H), 3.90 (s; 3 H), 3.35 (s; 2 H), 3.22 (s; 3 H), 2.94 (s; 3 H), 2.54 (d; J = 9.3; 1 H), 2.46 (s; 2 H), 2.29 (s; 2 H), 2.08 (s; 4 H), 2.03 (d; J = 10.8; 1 H), 2.00 (s; 3 H), 1.98 (s; 3 H), 1.53 (d; J = 11.1; 1 H) and 1.32 (d; J = 9.3 Hz; 1 H). UV/visible spectrum {CH_3CN; λ_{max}/nm ($10^{-4}\varepsilon$/M^{-1} cm^{-1}}: 251 (5.85), 276 (7.00), 285 (6.61), 435(sh) (142) and 451 (1.57). Electrochemistry $[(n\text{-}C_4H_9)_4N]ClO_4$; platinum working electrode; reference Ag–Ag^+}, $E_{1/2}$ = 0.995, −0.975 V. Complex **6**: yield 13.5 mg (47%). Accurate mass: observed *m*/*z* 1613.3252 (most abundant isotope peak within cluster), $[RuC_{80}H_{66}N_6O_{16}(PF_6)]^+$ requires 1613.3244. ^{1}H NMR (300 MHz, CD_3CN): δ 8.83–8.77 (m; 2 H), 8.54–8.44 (m; 4 H), 8.11–7.94 (m; 8 H), 7.83–7.63 (m; 6 H), 7.50–7.37 (m; 4 H), 7.25–7.16 (m; 2 H), 3.88 (s; 6 H), 3.61 (s; 6 H), 3.33 (s; 2 H), 3.25 (s; 3 H), 3.00 (s; 3 H), 2.87 (m; 1 H), 2.79 (s; 2 H), 2.75 (m; 1 H), 2.71 (s; 2 H), 2.54 (d; J = 9.9; 1 H), 2.36 (m; 2 H), 2.24 (s; 2 H), 2.11 (s; 2 H), 1.99 (s; 3 H), 1.97 (s; 3 H) and 1.31 (d; J = 9.3 Hz; 1 H). UV/visible spectrum {CH_3CN; λ_{max}/nm ($10^{-4}\varepsilon$/M^{-1} cm^{-1}}: 251 (5.66), 275 (6.79), 285 (6.39), 435(sh) (1.39) and 451 (1.54). Electrochemistry {DPV; CH_3CN–0.1 M $[(n\text{-}C_4H_9)_4N]ClO_4$; platinum working electrode; reference Ag–Ag^+}, $E_{1/2}$ = 0.985, −0.980 V.

X-Ray crystallographic studies

Crystals of the ligand **1** suitable for structure determination

Table 2 Crystallographic details for the structural determination of the ligand **1**

Chemical formula	$C_{30}H_{28}N_2O_5$
Formula weight	496.56
Crystal system	Triclinic
Space group	$P\bar{1}$
a/Å	9.885(2)
b/Å	11.1965(7)
c/Å	13.035(1)
α/°	66.944(8)
β/°	86.00(1)
γ/°	65.86(1)
V/Å^3	1204.3(3)
Z	2
μ/mm^{-1}	0.09
No. reflections collected	4219
No. observed reflections	2677
R	0.055
R_w	0.061

were grown *via* slow evaporation of a methanol–chloroform solution. A unique room temperature diffractometer data set ($T \approx 295$ K; monochromatic Mo-Kα radiation, $\lambda = 0.71073$ Å; 2θ–θ scan mode) was measured on an Enraf-Nonius CAD4 diffractometer, yielding 4219 independent reflections, 2677 with $I > 3\sigma(I)$ being considered 'observed' and used in the large block least squares refinements. Anisotropic thermal parameters were refined for all non-hydrogen atoms. Hydrogen atoms were placed in calculated positions and not refined. Neutral atom complex scattering factors were employed, and ring computation was by the XTAL 3.4 program system, implemented by S. R. Hall.[43] Crystallographic details are provided in Table 2.

CCDC reference number 186/2030.

See http://www.rsc.org/suppdata/dt/b0/b003174g/ for crystallographic files in .cif format.

Acknowledgements

This work was funded by the Australian Research Council. We thank Dr Ian Atkinson (James Cook University) for assistance with the molecular modelling calculations, and Mr Tom Frey (Central Queensland University) for the HR-MS analyses.

References

1 (*a*) K. Kumar, R. J. Tepper, Y. Zeng and M. B. Zimmt, *Tetrahedron*, 1995, **51**, 9241; (*b*) K. Kumar, Z. Lin, D. H. Waldeck and M. B. Zimmt, *J. Am. Chem. Soc.*, 1996, **118**, 243; (*c*) J. M. Lawson, D. C. Craig, A. M. Oliver and M. N. Paddon-Row, *Tetrahedron*, 1995, **51**, 3841; (*d*) M. N. Paddon-Row and M. J. Shephard, *J. Am. Chem. Soc.*, 1997, **119**, 5355.
2 V. Balzani, A. Juris, M. Venturi, S. Campagna and S. Serroni, *Chem. Rev.*, 1996, **96**, 759.
3 M. R. Wasielewski, *Chem. Rev.*, 1992, **92**, 435; D. Gust, T. A. Moore and A. L. Moore, *Acc. Chem. Res.*, 1993, **26**, 198.
4 V. Balzani and F. Scandola, *Supramolecular Photochemistry*, Ellis Horwood, Chichester, 1991.
5 A. C. Benniston, P. R. Mackie and A. Harriman, *Angew. Chem., Int. Ed.*, 1998, **37**, 354.
6 T. J. Rutherford and F. R. Keene, *Inorg. Chem.*, 1997, **36**, 2872; J. A. Treadway, P. Chen, T. J. Rutherford, F. R. Keene and T. J. Meyer, *J. Phys. Chem. A*, 1997, **101**, 6824.
7 J.-P. Sauvage, J.-P. Collin, J.-C. Chambron, S. Guillerez, C. Coudret, V. Balzani, F. Barigelletti, L. De Cola and L. Flamigni, *Chem. Rev.*, 1994, **94**, 993; J.-P. Collin, P. Gavina, V. Heitz and J.-P. Sauvage, *Eur. J. Inorg. Chem.*, 1998, 1; M. T. Indelli, F. Scandola, J.-P. Collin, J.-P. Sauvage and A. Sour, *Inorg. Chem.*, 1996, **35**, 303; A. Harriman and R. Ziessel, *Chem. Commun.*, 1996, 1707; D. Tzalis and Y. Tor, *J. Am. Chem. Soc.*, 1997, **119**, 852; M. T. Indelli, F. Scandola, L. Flamigni, J.-P. Collin, J.-P. Sauvage and A. Sour, *Inorg. Chem.*, 1997, **36**, 4247; A. C. Benniston, A. Harriman, V. Grosshenny and R. Ziessel, *New J. Chem.*, 1997, **21**, 405.
8 K. Warnmark, J. A. Thomas, O. Heyke and J.-M. Lehn, *Chem. Commun.*, 1996, 701; S. Bodige, A. S. Torres, D. J. Maloney, D. Tate, G. R. Kinsel, A. K. Walker and F. M. MacDonnell, *J. Am. Chem. Soc.*, 1997, **119**, 10364.
9 L. S. Kelso, D. A. Reitsma and F. R. Keene, *Inorg. Chem.*, 1996, **35**, 5144.
10 T. J. Rutherford, O. Van Gijte, A. Kirsch-De Mesmaeker and F. R. Keene, *Inorg. Chem.*, 1997, **36**, 4465.
11 (*a*) S. Bernhard and P. Belser, *Synthesis*, 1996, 192; (*b*) V. Balzani, F. Barigelletti, P. Belser, S. Bernhard, L. De Cola and L. Flamigni, *J. Phys. Chem.*, 1996, **100**, 16786.
12 (*a*) K. D. Jordan and M. N. Paddon-Row, *Chem. Rev.*, 1992, **92**, 395; (*b*) J. M. Lawson, M. N. Paddon-Row, W. Schuddeboom, J. M. Warman, A. H. A. Clayton and K. P. Ghiggino, *J. Phys. Chem.*, 1993, **97**, 13099; (*c*) M. N. Paddon-Row, *Acc. Chem. Res.*, 1994, **27**, 18.
13 P. T. Gulyas, S. J. Langford, N. R. Lokan, N. G. Ranasinghe and M. N. Paddon-Row, *J. Org. Chem.*, 1997, **62**, 3038.
14 (*a*) R. N. Warrener, A. B. B. Ferreira, A. C. Schultz, D. N. Butler, F. R. Keene and L. S. Kelso, *Angew. Chem., Int. Ed. Engl.*, 1996, **35**, 2485; (*b*) R. N. Warrener, M. A. Houghton, A. C. Schultz, F. R. Keene, L. S. Kelso, R. Dash and D. N. Butler, *Chem. Commun.*, 1996, 1151; (*c*) R. N. Warrener, A. C. Schultz, M. A. Houghton and D. N. Butler, *Tetrahedron*, 1997, **53**, 3991.
15 L. De Cola, V. Balzani, F. Barigelletti, L. Flamigni, P. Belser and S. Bernhard, *Recl. Trav. Chim. Pays-Bas*, 1995, **114**, 534.
16 A. Golka, P. J. Keyte and M. N. Paddon-Row, *Tetrahedron*, 1992, **48**, 7633; A. Golka, D. C. Craig and M. N. Paddon-Row, *Aust. J. Chem.*, 1994, **47**, 101.
17 P. T. Gulyas, T. A. Smith and M. N. Paddon-Row, *J. Chem. Soc., Dalton Trans.*, 1999, 1325.
18 A. C. Schultz, L. S. Kelso, M. R. Johnson, R. N. Warrener and F. R. Keene, *Inorg. Chem.*, 1999, **38**, 4906.
19 A. C. Schultz, PhD Thesis, Central Queensland University, 1998.
20 H. Taube, *Surv. Prog. Chem.*, 1974, **6**, 1.
21 A. Juris, F. Barigelletti, S. Campagna, V. Balzani, P. Belser and A. von Zelewsky, *Coord. Chem. Rev.*, 1988, **84**, 85.
22 J. M. Lawson, A. M. Oliver, D. F. Rothenfluh, Y.-Z. An, G. A. Ellis, M. G. Ranasinghe, S. I. Khan, A. G. Franz, P. S. Ganapathi, M. J. Shephard, M. N. Paddon-Row and Y. Rubin, *J. Org. Chem.*, 1996, **61**, 5032.
23 C. K. Johnson, ORTEP II, Report ORNL-5138, Oak Ridge National Laboratory, Oak Ridge, TN, 1976.
24 R. J. Cave, M. D. Newton, K. Kumar and M. B. Zimmt, *J. Phys. Chem.*, 1995, **99**, 17501.
25 D. Margetic, M. R. Johnston, E. R. T. Tiekink and R. N. Warrener, *Tetrahedron Lett.*, 1998, **29**, 5277.
26 J. Fees, W. Kaim, M. Moscherosch, W. Matheis, J. Klíma, M. Krejcík and S. Zális, *Inorg. Chem.*, 1993, **32**, 166.
27 R. B. Nair, B. M. Culllum and C. J. Murphy, *Inorg. Chem.*, 1997, **36**, 962.
28 J. A. Treadway, B. Loeb, R. Lopez, P. A. Anderson, F. R. Keene and T. J. Meyer, *Inorg. Chem.*, 1996, **35**, 2242.
29 A. Weller, *Z. Phys. Chem.*, 1982, **133**, 93.
30 H. Han and M. B. Zimmt, *J. Am. Chem. Soc.*, 1998, **120**, 8001.
31 K. Kim, K. D. Jordan and M. N. Paddon-Row, *J. Phys. Chem.*, 1994, **98**, 11053.
32 V. Balaji, L. Ng, K. D. Jordan, M. N. Paddon-Row and H. K. Patney, *J. Am. Chem. Soc.*, 1987, **109**, 6957.
33 N. J. Turro, *Modern Photochemistry*, Benjamin, Menlo Park, CA, 1978.
34 S. Nakatsuji, T. Yahiro, K. Nakashima, S. Akiyama and H. Nakazumi, *Bull. Chem. Soc. Jpn.*, 1991, **64**, 1641; G. Giuffrida, G. Calogero, G. Guglielmo, V. Ricevuto and S. Campagna, *Inorg. Chim. Acta*, 1996, **251**, 255; L. De Cola, V. Balzani, F. Barigelletti, L. Flamigni, P. Belser, A. von Zelewsky, M. Frank and F. Vögtle, *Inorg. Chem.*, 1993, **32**, 5228.
35 *Resonance Energy Transfer: Theory and Data*, eds. B. Wieb van der Meer, G. Coker and S. Y. S. Chen, VCH, New York, 1994.
36 M. Furue, T. Yoshdzumi, S. Kinoshita, T. Kushida, S. Nozakura, and M. Kamachi, *Bull. Chem. Soc. Jpn.*, 1991, **64**, 1632.
37 B. Schlicke, P. Besler, L. De Cola, E. Sabbioni and V. Balzani, *J. Am. Chem. Soc.*, 1999, **121**, 4207.
38 SPARTAN v 5.0, Wavefunction, Inc., Irvine, CA, 1997.
39 R. N. Warrener, and D. N. Butler, *Aldrichim. Acta*, 1997, **30**, 119.
40 R. N. Warrener, A. C. Schulz, D. N. Butler, S. Wang, I. B. Mahadevan and R. A. Russell, *Chem. Commun.*, 1997, 1023.
41 M. J. Ridd, D. J. Gakowski, G. E. Sneddon and F. R. Keene, *J. Chem. Soc., Dalton Trans.*, 1992, 1949.
42 L. A. Paquette, F. Bellamy, M. C. Bohm and R. J. Gleiter, *J. Org. Chem.*, 1980, **45**, 4913.
43 S. R. Hall, G. S. D. King and J. M. Stewart, *XTAL 3.4 User's Manual*, University of Western Australia, Lamb, Perth, 1995.